Supporting Information

Evaluation of the role of superoxide as chain carrier of ozone decomposition to hydroxyl radicals during ozonation

Yang Guo[a], Gang Yu[a], Urs von Gunten [b,c], Yujue Wang[a*]

[a] School of Environment, Beijing Key Laboratory for Emerging Organic Contaminants Control, State Key Joint Laboratory of Environmental Simulation and Pollution Control, Tsinghua University, Beijing 100084 China.

[b] Eawag, Swiss Federal Institute of Aquatic Science and Technology, CH-8600 Dübendorf, Switzerland

[c] School of Architecture, Civil and Environmental Engineering (ENAC), Ecole Polytechnique Fédérale Lausanne (EPFL), CH-1015 Lausanne, Switzerland

[*] Corresponding author. E-mail: wangyujue@tsinghua.edu.cn (Yujue Wang)

S1. Composition of synthetic solutions

Table S1. Composition of synthetic solutions used in this study (buffered with 10 mM phosphate at pH = 8) with the concentrations and the first-order scavenging rate constants. The second-order rate constants for the reaction of methanol, acetate, and *tert*-butanol with •OH are 9.7×10^8 M^{-1} s^{-1}, 7.9×10^7 M^{-1} s^{-1}, and 5×10^8 M^{-1} s^{-1}, respectively. (Buxton et al., 1988; Wolfenden and Willson, 1982)

Solution	Methanol		Acetate		*tert*-Butanol		Overall •OH scavenging rate (s^{-1})
	[C] (M)	$k_{\bullet OH}[C]$ (s^{-1})	[C] (M)	$k_{\bullet OH}[C]$ (s^{-1})	[C] (M)	$k_{\bullet OH}[C]$ (s^{-1})	
1	1.24×10^{-4}	1.2×10^5	0	0	0	0	1.2×10^5
2	0.93×10^{-4}	0.9×10^5	0.38×10^{-3}	0.3×10^5	0	0	1.2×10^5
3	0.62×10^{-4}	0.6×10^5	0.76×10^{-3}	0.6×10^5	0	0	1.2×10^5
4	0.31×10^{-4}	0.3×10^5	1.14×10^{-3}	0.9×10^5	0	0	1.2×10^5
5	0	0	1.52×10^{-3}	1.2×10^5	0	0	1.2×10^5
6	0.93×10^{-4}	0.9×10^5	0	0	0.6×10^{-4}	0.3×10^5	1.2×10^5
7	0.62×10^{-4}	0.6×10^5	0	0	1.2×10^{-4}	0.6×10^5	1.2×10^5
8	0.31×10^{-4}	0.3×10^5	0	0	1.8×10^{-4}	0.9×10^5	1.2×10^5
9	0	0	0	0	2.4×10^{-4}	1.2×10^5	1.2×10^5

S2. Determination of the second-order rate constant for the reaction of $O_2^{\bullet-}$ with acetate

The second-order rate constant for the reaction of $O_2^{\bullet-}$ with acetate ($k_{O_2^{\bullet-},ACT}$) was measured by competition kinetics in a xanthine-xanthine oxidase (XOD) system (Guo et al., 2021b; Pasternack and Halliwell, 1979). The system (3 mL) contained xanthine (400 μM), XOD (0.2 U) and DETAPAC (1 mM). The reference compound was nitrotetrazolium blue chloride (NBT), which reacts with $O_2^{\bullet-}$ with a second-order rate constant of 6×10^4 M^{-1} s^{-1}. The reaction of $O_2^{\bullet-}$ with NBT^{2+} yields the stable and colored formazan, for which the concentrations was measured by spectrophotometry (Hach DR6000, USA) at λ=560 nm (ε = 13800 $M^{-1}cm^{-1}$).

In the experiments where the test compound (M) was added togther with the NBT^{2+} to the xanthine and XOD system, the generated $O_2^{\bullet-}$ were mainly consumed in the parallel reactions with NBT^{2+} and M

$$NBT^{2+} + O_2^{\bullet-} \xrightarrow{k_{O_2^{\bullet-},\,NBT^{2+}}} \text{Formazan} + O_2 \qquad \text{(S1)}$$

$$M + O_2^{\bullet-} \xrightarrow{k_{O_2^{\bullet-},\,M}} M' + O_2 \qquad \text{(S2)}$$

where M and M' are the test compound and the product from the reaction of $O_2^{\bullet-}$ with M, respectively; $k_{O_2^{\bullet-},\,M}$ is the second-order rate constant for the reaction of $O_2^{\bullet-}$ with M. Assuming a steady-state approximation to $O_2^{\bullet-}$, we can obtain

$$\frac{d[O_2^{\bullet-}]}{dt} = 0 = r - k_{O_2^{\bullet-},\,NBT^{2+}}[NBT^{2+}][O_2^{\bullet-}] - k_{O_2^{\bullet-},\,M}[M][O_2^{\bullet-}] \qquad \text{(S3)}$$

where r is the rate of $O_2^{\bullet-}$ production from the enzymatically catalyzed reaction of xanthine with XOD. By rearranging Eq. S3, the concentration of $O_2^{\bullet-}$ is given as

$$[O_2^{\bullet-}] = \frac{r}{k_{O_2^{\bullet-},\,NBT^{2+}}[NBT^{2+}] + k_{O_2^{\bullet-},\,M}[M]} \qquad \text{(S4)}$$

Meanwhile, the rate of formazan production (v) from Eq. S1 can be expressed as

$$v = \frac{d[\text{formazan}]}{dt} = k_{O_2^{\bullet-},\,NBT^{2+}}[NBT^{2+}][O_2^{\bullet-}] \qquad \text{(S5)}$$

By substituting Eq. S4 into Eq. S5, we obtain

$$v = \frac{d[\text{formazan}]}{dt} = r \bullet \frac{k_{O_2^{\bullet-},\,NBT^{2+}}\,[NBT^{2+}]}{k_{O_2^{\bullet-},\,NBT^{2+}}\,[NBT^{2+}] + k_{O_2^{\bullet-},\,M}\,[M]} \quad \text{(S6)}$$

In the experiment where only the reference compound (NBT^{2+}) was added in the system (no test compound was added), Eq. S3 changes to

$$\frac{d[O_2^{\bullet-}]}{dt} = 0 = r - k_{O_2^{\bullet-},\,NBT^{2+}}\,[NBT^{2+}][O_2^{\bullet-}] \quad \text{(S7)}$$

and the rate of formazan production (V) in the absence of M is given as

$$V = \frac{d[\text{formazan}]}{dt} = k_{O_2^{\bullet-},\,NBT^{2+}}\,[NBT^{2+}][O_2^{\bullet-}] \quad \text{(S8)}$$

Combining Eq. S7 and S8, we obtain

$$r = V \quad \text{(S9)}$$

Finally, by substituting Eq. S9 into Eq. S6 and rearranging the obtained equation, we can get

$$\frac{V}{v} = \frac{k_{O_2^{\bullet-},\,M}\,[M]}{k_{O_2^{\bullet-},\,NBT^{2+}}\,[NBT^{2+}]} + 1 \quad \text{(S10)}$$

Therefore, by following the production rate of formazan in the absence and presence of M (V and v), the second-order rate constant for the reaction of $O_2^{\bullet-}$ with the test compound can be estimated from the slope of linear regression of Eq. S10. (Guo et al., 2021b; Pasternack and Halliwell, 1979). As shown in Fig. S1, the slope of the regression line represents the $k_{O_2^{\bullet-}}$ ratio between target compound and NBT^{2+} (Eq. (S10)). Based on the $k_{O_2^{\bullet-},\,NBT^{2+}}$, the second-order rate constant for the reaction of $O_2^{\bullet-}$ with acetate was determined as $3.2 \times 10^4\ M^{-1}\ s^{-1}$.

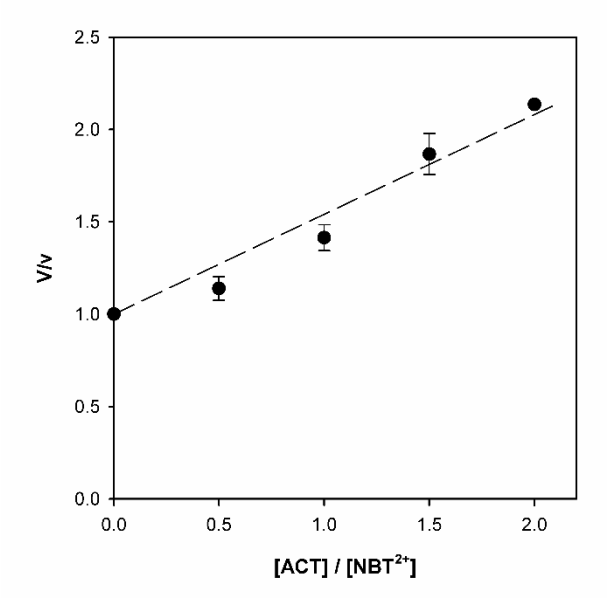

Fig. S1. Determination of the second-order rate constant for the reaction of acetate with $O_2^{\bullet-}$. Ratio of production rate of the reference compound (NBT^{2+}) as a function of molar ratios of acetate and NBT^{2+}. Reaction conditions: [NBT^{2+}] = 1 mM, [Acetate] = 0.5, 1.0, 1.5, and 2 mM.

S3. Reaction of CCl_4 with $O_2^{\bullet-}$

The second-order rate constant for the reaction of CCl_4 with $O_2^{\bullet-}$ has been determined to be 1.1×10^9 M^{-1} s^{-1} in a previous study using the same method as described in Text S1 (Guo et al., 2021a). In the present study, the second-order rate constant for the reaction of $O_2^{\bullet-}$ with CCl_4 was further verified using the competition kinetic method with 2,5-dichloro-*p*-benzoquinone ($k_{O_2^{\bullet-}}$ = 1.1×10^9 M^{-1} s^{-1} (Bielski et al., 1985)) as the reference compound. As shown in Fig. S2a, the concentration of CCl_4 decreased only slightly slower than that of 2,5-dichloro-*p*-benzoquinone in the xanthine-xanthine oxidase system. After 20 min, the concentration of CCl_4 was abated by ~20% in the system. Although the decreases of CCl_4 concentrations are relatively small under the tested reaction conditions, they can still provide a valid estimation of the second-order rate constant. Based on the linear regression between the natural logarithm of the relative residual concentrations of CCl_4 and chlorobenzoquinone (Fig. S2a inset), the second-order rate constant for the reaction of $O_2^{\bullet-}$ with CCl_4 was determined as

8.4×10^8 M^{-1} s^{-1}, which is very close to the previously reported value (within the experimental errors). This result confirms that CCl_4 can react rapidly with $O_2^{\bullet-}$, and the previously reported rate constant is reliable. Note that loss of CCl_4 through evaporation was evaluated in pure water and found to be negligible under the tested conditions (Fig. S2b).

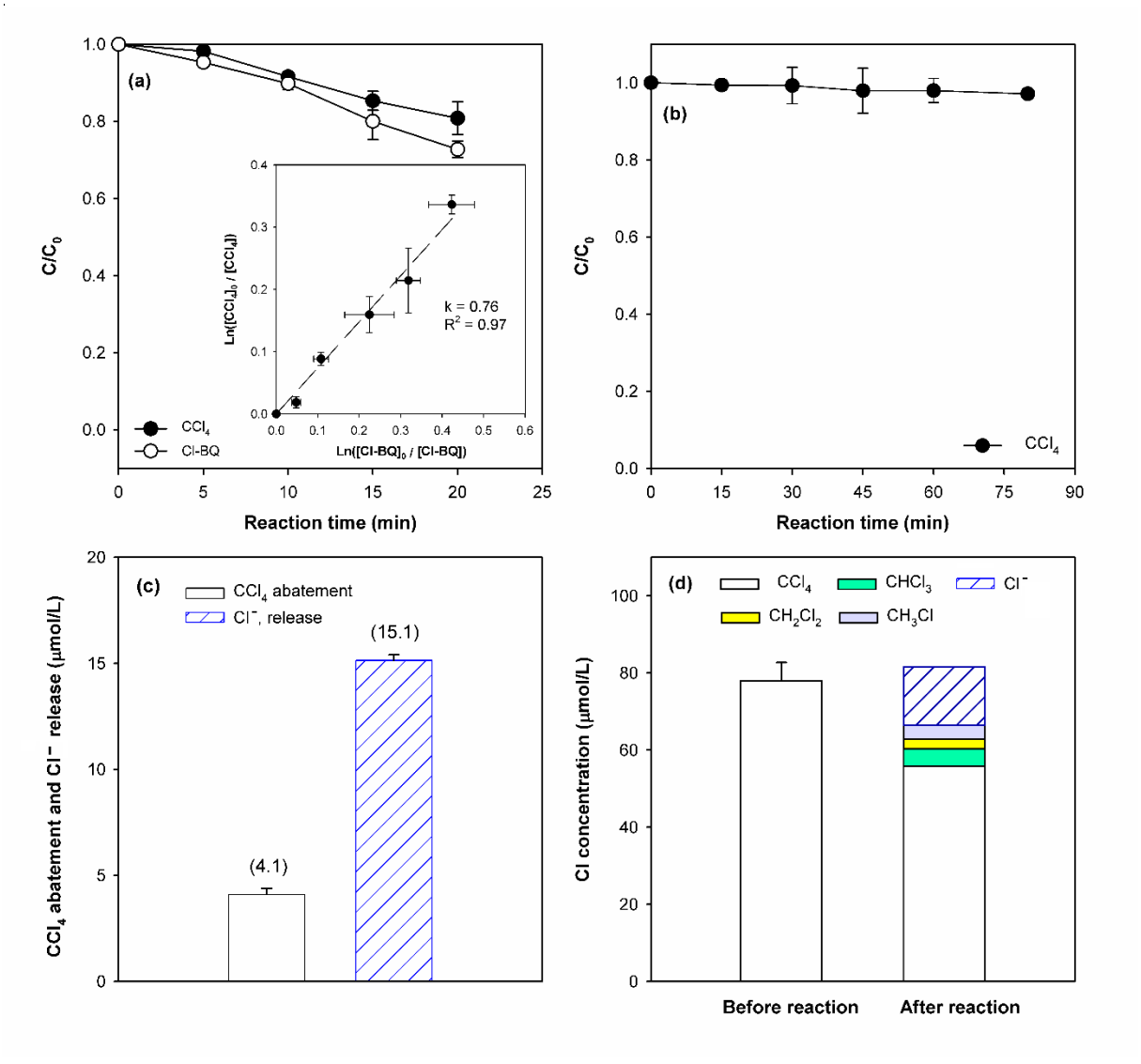

Fig. S2. Determination of the kinetics of the reaction between $O_2^{\bullet-}$ and CCl4. (a) Decrease of CCl_4 and 2,5-dichloro-*p*-benzoquinone concentrations in the xanthine-xanthine oxidase system; (b) blank experiment to test the stability of CCl_4 concentrations in water; (c) degraded CCl_4 and released Cl^- during the xanthine-xanthine oxidase process; (d) chlorine concentration balance before and after the xanthine-xanthine oxidase process. Experimental conditions: (a) $[CCl_4]$ = [2,5-dichloro-p-benzoquinone]$_0$ = 200 μg/L, [xanthine] = 400 μM, [XOD] = 0.3 U,

pH = 8.0 (phosphate buffered); (b) $[CCl_4]_0$ = 200 μg/L; (c, d) $[CCl_4]_0$ = 20 μM (~3 mg/L), [xanthine] = 800 μM, [XOD] = 0.8 U, pH = 8.0 (phosphate buffered).

To examine dechlorination of CCl_4 by $O_2^{\bullet-}$, 20 μM CCl_4 was added in the xanthine-xanthine oxidase system. After the reaction was completed, approximately 4.1 μM CCl_4 was degraded, while 15.1 μM Cl^- was detected in the system. These data suggest that on average, 3.68 moles of Cl^- are released per mole of CCl_4 degraded during the reaction. Meanwhile, dechlorination transformation products of CCl_4 ($CHCl_3$, CH_2Cl_2, and CH_3Cl) were detected in the water, yielding a good overall molar Cl balance (Fig. S2c). The results observed herein are in agreement with the previous findings that $O_2^{\bullet-}$ is a strong nucleophile and can degrade chlorinated organics through a nucleophilic substitution mechanism (Hayyan et al., 2016; Mitchell et al., 2014; Smith et al., 2004).

S4. Ozone decomposition in the presence of CCl_4

Fig. S3 shows that with increasing CCl_4 concentrations, the rate of O_3 depletion decreased considerably during ozonation. This change can be mainly attributed to an enhanced suppression of the $O_2^{\bullet-}$-promoted O_3 decomposition at higher CCl_4 concentrations. For the highest concentration of CCl_4 (6.3 mM), the observed pseudo-first order rate of O_3 depletion was 1.9×10^{-3} s^{-1}, which is about three times the rate of O_3 depletion caused by the reaction with OH^- at pH 9 ($k = 7 \times 10^{-4}$ s^{-1}). This difference suggests that the $O_2^{\bullet-}$-promoted O_3 decomposition is not fully suppressed at the applied CCl_4 concentration, or there are some impurities in the synthetic solutions that may initiate the O_3 decomposition (e.g., chemicals and buffers added in the synthetic solutions may contain some impurities that can react with O_3).

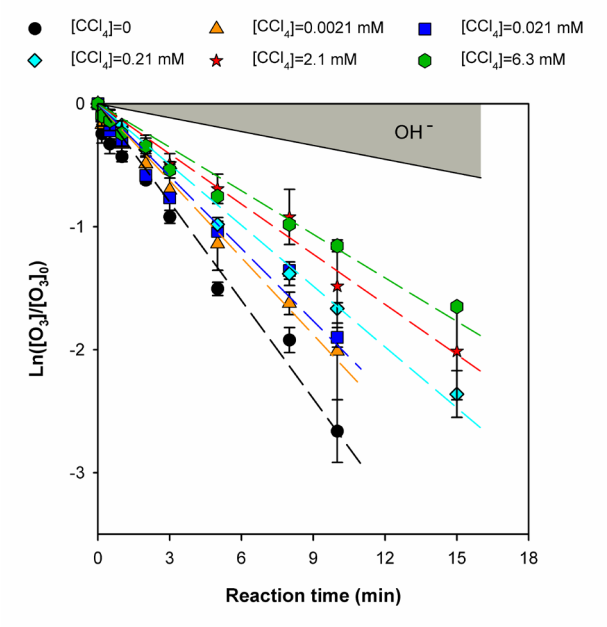

Fig. S3. Ozone decomposition kinetics in synthetic solutions containing varying concentrations of CCl_4. Reaction condition: O_3 dose = 1.0 mg/L (0.021 mM), [CCl_4] = 0.0021–6.3 mM, pH = 9 (buffered with 10 mM borate). The line of O_3 depletion by the reaction with OH^- is simulated using a second-order rate constant of 70 M^{-1} s^{-1} (Merényi et al., 2010).

S5. Methanol and acetate as a chain promoter and inhibitor, respectively

Fig. S4 shows the evolution of O_3, $^{\bullet}OH$, and $O_2^{\bullet-}$ concentrations during ozonation of synthetic solutions with constant total scavenging rate and various scavenging ratios of promotor (methanol)/inhibitor (acetate) (see Table 1).

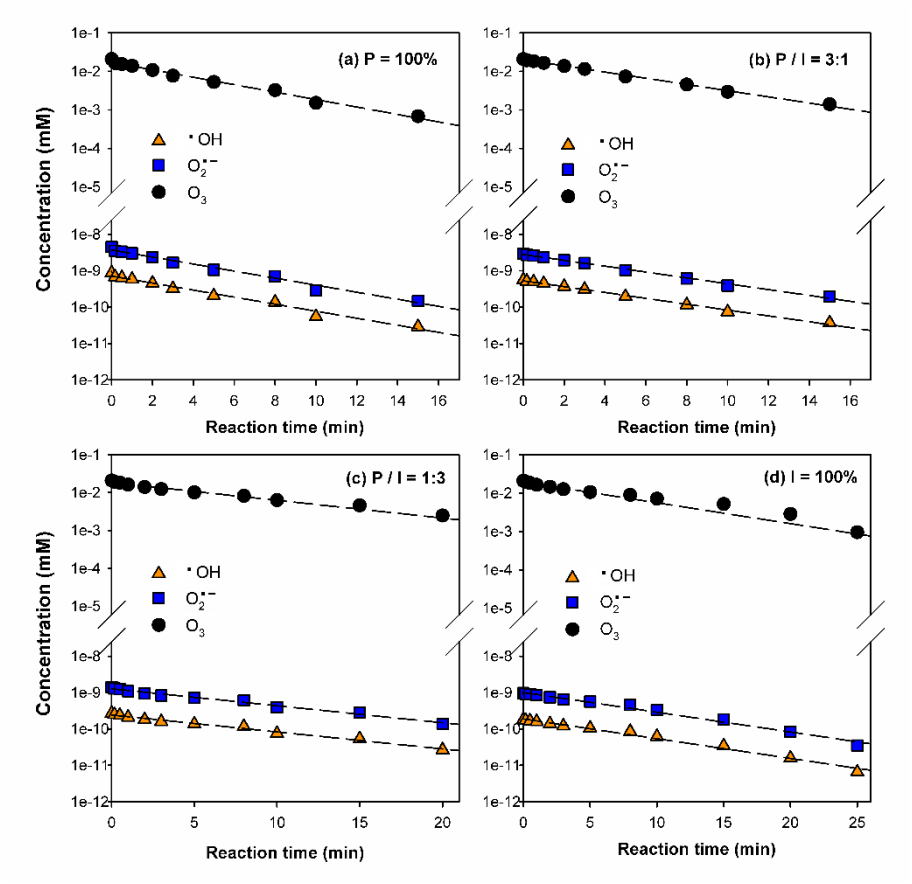

126

127 **Fig. S4.** Evolution of O_3, $^{\bullet}OH$, and $O_2^{\bullet-}$ concentrations for various promotor (P):inhibitor (I)
128 scavenging ratios (P/I). (a) P = 100%, (b) P/I = 3:1, (c) P/I = 1:3 and (d) I = 100% during
129 ozonation. Reaction conditions: O_3 dose = 0.021 mM, pH ~8.0 (phosphate buffer, 10 mM),
130 total scavenging rate = 1.2×10^5 s^{-1}, P =100%: [MeOH] = 0.124 mM; P/I = 3: [MeOH] = 0.093
131 mM, [Acetate] = 0.38 mM; P/I = 1/3: [MeOH] = 0.031 mM, [Acetate] = 1.14 mM; I =100%:
132 [Acetate] = 1.52 mM.

133

134

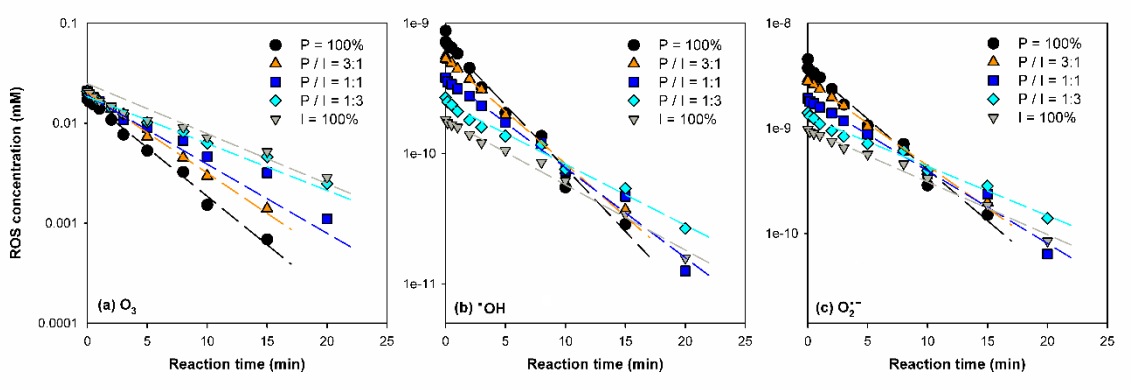

135

136 **Fig. S5.** Effects of the P/I ratios on the evolution of (a) O_3, (b) •OH, and (c) $O_2^{\bullet-}$ concentrations
137 during ozonation of MeOH- and/or acetate-containing solutions. Reaction condition: O_3 dose
138 = 0.021 mM, [MeOH] = 0–0.124 mM, [acetate] = 0–1.14 mM, pH ~8.0 (phosphate buffer, 10
139 mM), total scavenging rate = 1.2×10^5 s^{-1}, P =100%: [MeOH] = 0.124 mM; P/I = 3: [MeOH]
140 = 0.093 mM, [acetate] = 0.38 mM; P/I = 1: [MeOH] = 0.062 mM, [acetate] = 0.76 mM; P/I =
141 1/3: [acetate] = 0.031 mM, [acetate] = 1.14 mM; I =100%: [acetate] = 1.52 mM.

142

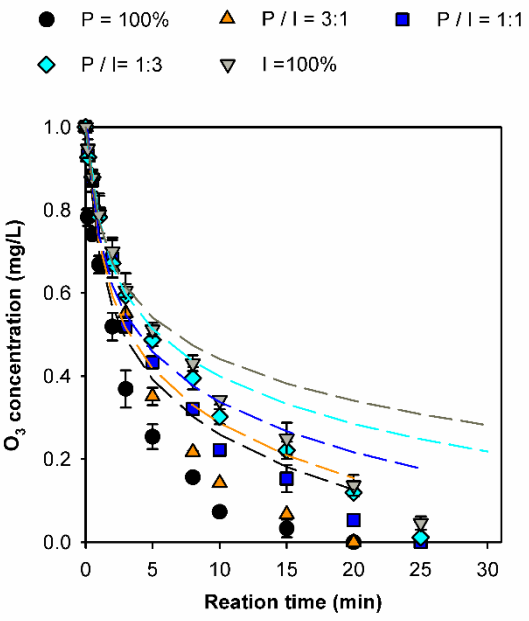

143

144 **Fig. S6.** Modelling of ozone decomposition in MeOH- and /or acetate-containing solutions by
145 Eq. 15 ($k_{\bullet OH, O_3}$ = 1.1×10^8 M^{-1} s^{-1}). The symbols are experimental and the dashed lines
146 modelling results. Reaction condition: O_3 dose = 0.021mM, pH ~8.0 (phosphate buffer, 10

147 mM), total scavenging rate = 1.2×10^5 s^{-1}, P =100%: [MeOH] = 0.124 mM, P/I = 3: [MeOH]
148 = 0.093 mM, [acetate] = 0.38 mM; P/I = 1: [MeOH] = 0.062 mM, [acetate] = 0.76 mM; P/I =
149 1/3: [MeOH] = 0.031 mM, [acetate] = 1.14 mM; I =100%: [acetate] = 1.52 mM.
150
151 **S6. Methanol and *tert*-butanol as a chain promoter and inhibitor, respectively**
152 The results obtained with *tert*-butanol as an inhibitor (Fig. S6) were generally very similar
153 to those obtained with acetate (Fig. 1).

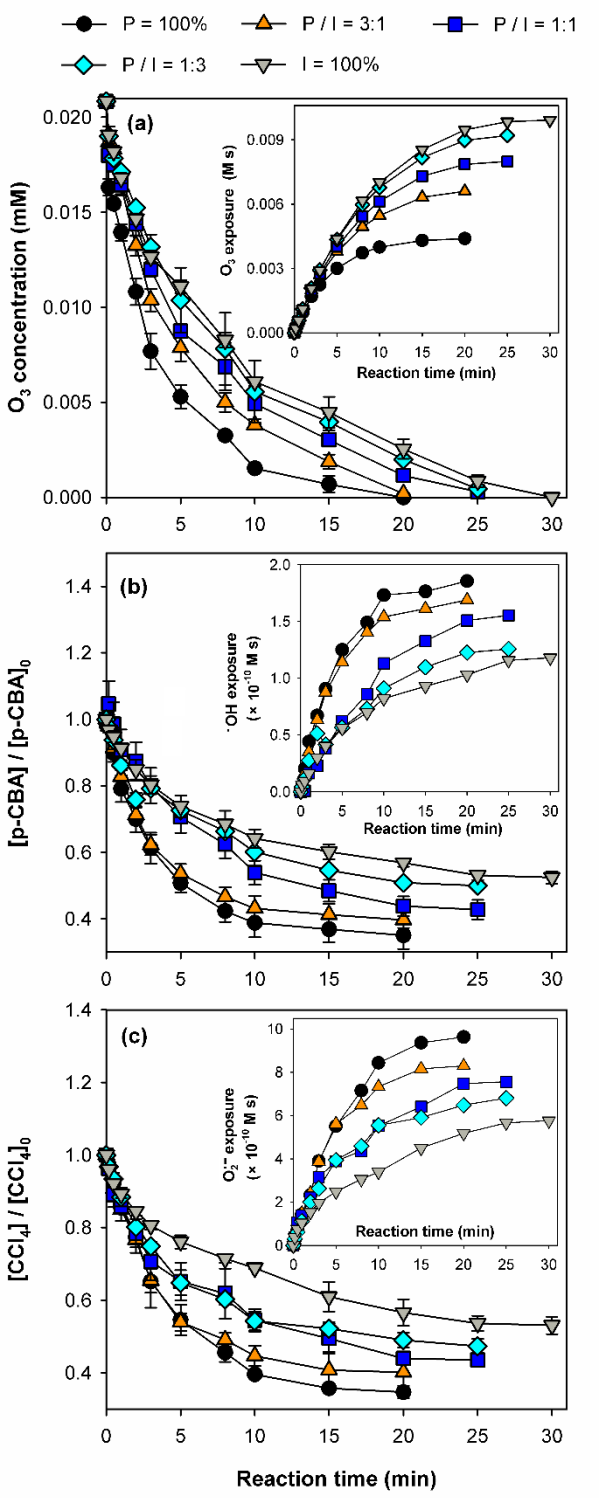

154

155 **Fig. S7.** Ozonation of synthetic solutions with constant total scavenging rate and various
156 promotor (methanol):inhibitor (*tert*-butanol) scavenging ratios (P/I): Effect of the P/I ratios on
157 (a) ozone decrease, (b) *p*CBA abatement and (c) CCl_4 abatement during ozonation of MeOH-
158 and/or TBA-containing solutions. The insets in Fig. S6a, b and c show the O_3 exposures, $^{\bullet}OH$

159 exposures, and $O_2^{\bullet-}$ exposures, respectively. Reaction conditions: O_3 dose = 0.021mM, pH
160 ~8.0 (phosphate buffer, 10 mM), total scavenging rate = 1.2×10^5 s^{-1}, P =100%: [MeOH] =
161 0.124 mM; P/I = 3: [MeOH] = 0.093 mM, [TBA] = 0.06 mM; P/I = 1: [MeOH] = 0.062 mM,
162 [TBA] = 0.12 mM; P/I = 1/3: [MeOH] = 0.031 mM, [TBA] = 0.18 mM; I =100%: [TBA] =
163 0.24 mM.
164

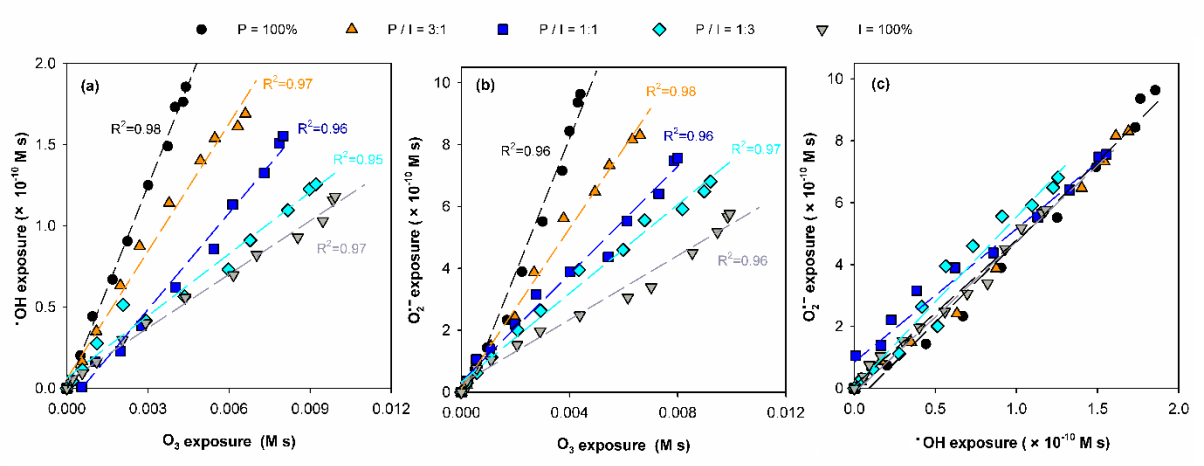

165

166 **Fig. S8.** Ozonation of synthetic solutions with constant total scavenging rate and various
167 promotor (methanol):inhibitor (*tert*-butanol) scavenging ratios (P/I): (a) R_{ct}, (b) R_{SO}, and (c)
168 R_{SH} as a function of the P/I ratios. Reaction conditions: O_3 dose = 0.021mM, pH ~8.0
169 (phosphate buffer, 10 mM), total scavenging rate = 1.2×10^5 s^{-1}. P =100%: [MeOH] = 0.124
170 mM; P/I = 3: [MeOH] = 0.093 mM, [TBA] = 0.06 mM; P/I = 1: [MeOH] = 0.062 mM, [TBA]
171 = 0.12 mM; P/I = 1/3: [MeOH] = 0.031 mM, [TBA] = 0.18 mM; I =100%: [TBA] = 0.24 mM.
172

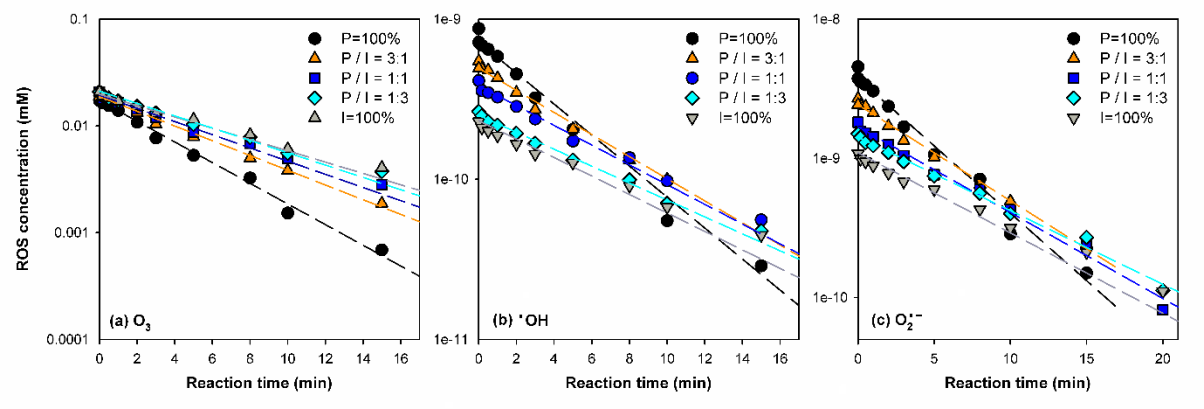

173

174 **Fig. S9.** Ozonation of synthetic solutions with constant total scavenging rate and various

175 promotor (methanol):inhibitor (*tert*-butanol) scavenging ratios (P/I): Effects of the P/I ratios

176 on the evolution of (a) O_3, (b) $^{\bullet}OH$, and (c) $O_2^{\bullet-}$ concentrations. Reaction conditions: O_3 dose

177 = 0.021mM, pH ~8.0 (phosphate buffer, 10 mM), total scavenging rate = 1.2×10^5 s^{-1}. P =100%:

178 [MeOH] = 0.124 mM; P/I = 3: [MeOH] = 0.093 mM, [TBA] = 0.06 mM; P/I = 1: [MeOH] =

179 0.062 mM, [TBA] = 0.12 mM; P/I = 1/3: [MeOH] = 0.031 mM, [TBA] = 0.18 mM; I =100%:

180 [TBA] = 0.24 mM.

181

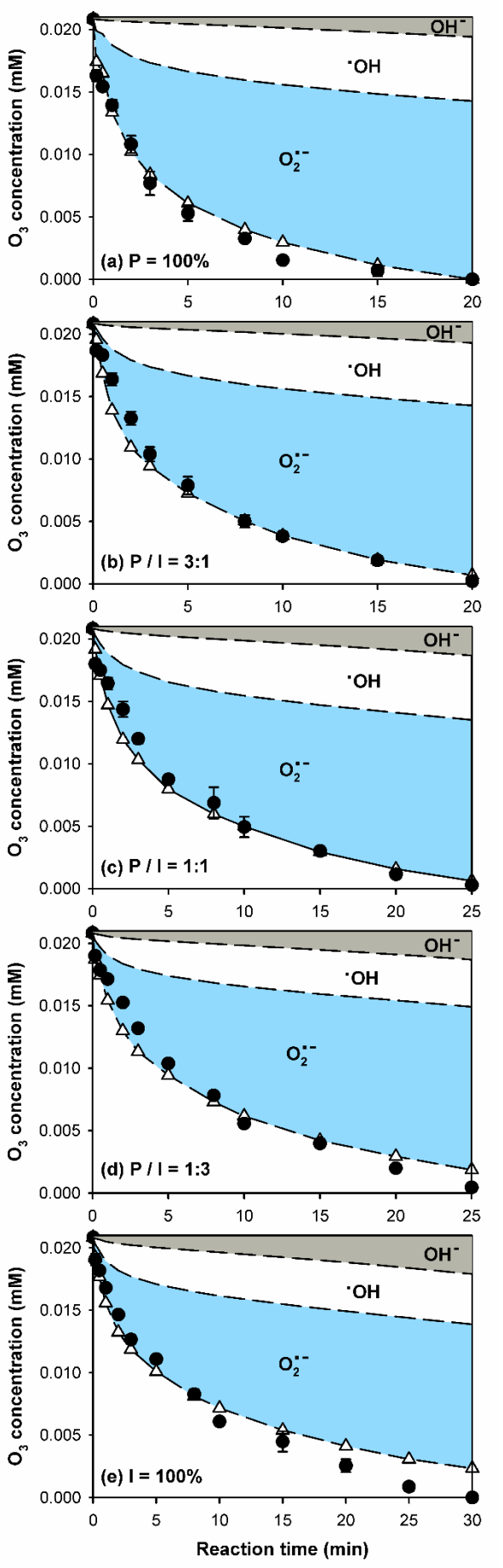
O_3 concentration (mM)
0.020
0.015
0.010
0.005
0.000
OH^-
$^{\bullet}OH$
$O_2^{\bullet-}$
(a) P = 100%
0
5
10
15
20
(b) P / I = 3:1
(c) P / I = 1:1
25
(d) P / I = 1:3
(e) I = 100%
30
Reaction time (min)

182

Fig. S10. Modelling of ozone decomposition in MeOH/TBA-containing solutions using Eq. 15 ($k_{^{\bullet}OH,O_3} = 3.0 \times 10^9\ M^{-1}\ s^{-1}$). The filled circles are experimental results, the open triangles are modelling results calculated using Eq. 15, and the dash lines are drawn based on the relative contribution of OH^-, $^{\bullet}OH$, and $O_2^{\bullet-}$, respectively, to the O_3 decay calculated by Eqs. 16-18. Reaction conditions: O_3 dose = 0.021mM, pH ~8.0 (phosphate buffer, 10 mM), total scavenging rate = $1.2 \times 10^5\ s^{-1}$. P =100%: [MeOH] = 0.124 mM; P/I = 3: [MeOH] = 0.093 mM, [TBA] = 0.06 mM; P/I = 1: [MeOH] = 0.062 mM, [TBA] = 0.12 mM; P/I = 1/3: [MeOH] = 0.031 mM, [TBA] = 0.18 mM; I =100%: [TBA] = 0.24 mM.

S7. Ozonation of natural waters

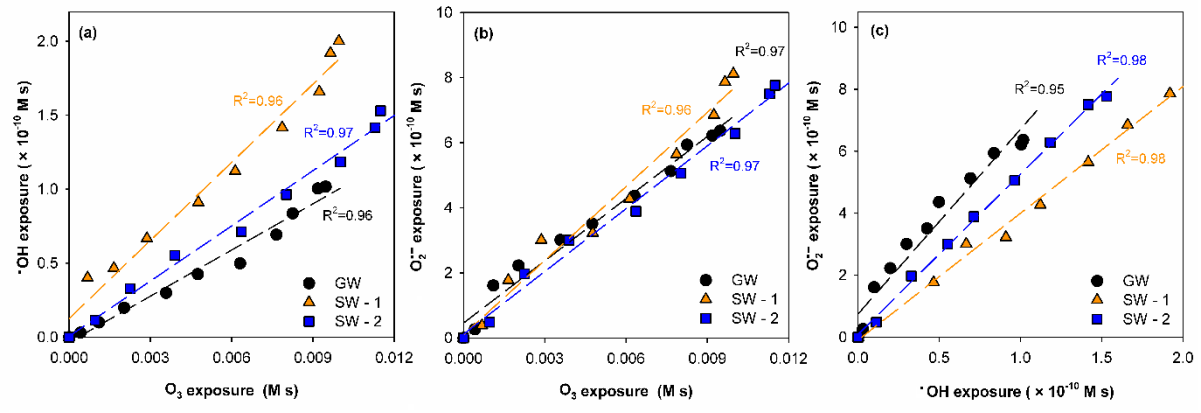

Fig. S11. Ozonation of a selected groundwater (GW) and two surface waters (SW-1, SW-2): (a) R_{ct}, (b) R_{SO}, and (c) R_{SH}. Reaction conditions: Specific O_3 dose = 1.0 mg O_3/mg DOC. For water quality data of the three real waters see Table 2.

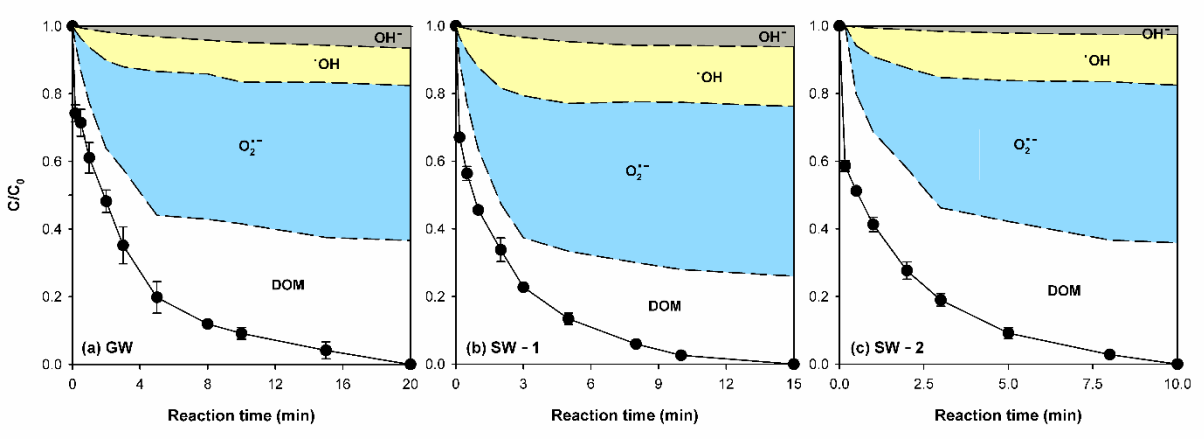

Fig. S12. Relative contribution of OH^-, $^{\bullet}OH$, $O_2^{\bullet-}$, and DOM to the relative ozone depletion (C/C_0) in the selected (a) groundwater (GW) and (b, c) surface waters (SW-1, SW-2). The solid circles are experimental data and the dash lines are drawn based on the relative contributions of OH^-, $^{\bullet}OH$, $O_2^{\bullet-}$, and DOM to O_3 decay calculated using Eqs. 21-24. Reaction conditions: Specific O_3 dose = 1.0 mg O_3/mg DOC. Refer to Table 2 for water quality data of the three real waters.

References

Bielski, B.H., Cabelli, D.E., Arudi, R.L. and Ross, A.B. 1985. Reactivity of HO2/O2-radicals in aqueous solution. J Phys Chem Ref Data 14(4), 1041-1100.

Buxton, G.V., Greenstock, C.L., Helman, W.P. and Ross, A.B. 1988. Critical Review of rate constants for reactions of hydrated electrons, hydrogen atoms and hydroxyl radicals (·OH/·O− in Aqueous Solution. J Phys Chem Ref Data 17(2), 513-886.

Guo, Y., Zhan, J., Yu, G. and Wang, Y. 2021a. Evaluation of the concentration and contribution of superoxide radical for micropollutant abatement during ozonation. Water Res 194, 116927.

Guo, Y., Zhang, Y., Yu, G. and Wang, Y. 2021b. Revisiting the role of reactive oxygen species for pollutant abatement during catalytic ozonation: The probe approach versus the scavenger approach. Applied Catalysis B: Environmental 280, 119418.

Hayyan, M., Hashim, M.A. and AlNashef, I.M. 2016. Superoxide Ion: Generation and Chemical Implications. Chem Rev 116(5), 3029-3085.

Merényi, G., Lind, J., Naumov, S. and von Sonntag, C. 2010. The Reaction of Ozone with the Hydroxide Ion: Mechanistic Considerations Based on Thermokinetic and Quantum Chemical Calculations and the Role of HO_4^- in Superoxide Dismutation. Chemistry – A European Journal 16(4), 1372-1377.

Mitchell, S.M., Ahmad, M., Teel, A.L. and Watts, R.J. 2014. Degradation of Perfluorooctanoic Acid by Reactive Species Generated through Catalyzed H_2O_2 Propagation Reactions. Environmental Science & Technology Letters 1(1), 117-121.

Pasternack, R.F. and Halliwell, B. 1979. Superoxide dismutase activities of an iron porphyrin and other iron complexes. J Am Chem Soc 101(4), 1026-1031.

Smith, B.A., Teel, A.L. and Watts, R.J. 2004. Identification of the reactive oxygen species responsible for carbon tetrachloride degradation in modified Fenton's systems. Environ Sci Technol 38(20), 5465-5469.

Wolfenden, B.S. and Willson, R.L. 1982. Radical-cations as reference chromogens in kinetic studies of ono-electron transfer reactions: pulse radiolysis studies of 2,2′-azinobis-(3-ethylbenzthiazoline-6-sulphonate). Journal of the Chemical Society, Perkin Transactions 2 (7), 805-812.